

A Low-Overhead Hierarchical Beam-tracking Algorithm for THz Wireless Systems

Giorgos Stratidakis*, Georgia D. Ntouni[†], Alexandros–Apostolos A. Boulogeorgos*,
Dimitrios Kritharidis[†], and Angeliki Alexiou*

*Department of Digital Systems, University of Piraeus, Piraeus 18534, Greece.

[†]Intracom Telecom, 19.7 km Markopoulou, Ave., 190 02 Peania, Greece.

E-mails: {giostrat, alexiou}@unipi.gr, {gntouni, dkri}@intracom-telecom.com, al.boulogeorgos@ieee.org.

Abstract—In this paper, a novel hierarchical beam-tracking approach, which is suitable for terahertz (THz) wireless systems, is presented. The main idea is to employ a prediction based algorithm with a multi-resolution codebook, in order to decrease the required overhead of tracking and increase its robustness. The efficiency of the algorithm is evaluated in terms of the average number of pilots and mean square error (MSE) and is compared with the corresponding performance of the fast channel tracking (FCT) algorithm. Our results highlight the superiority of the proposed approach in comparison with FCT, in terms of tracking efficiency with low overhead.

Index Terms—THz wireless, Beamforming, Beam-tracking, Hierarchical codebook.

I. INTRODUCTION

The key enabling technology for wireless terahertz (THz) communications is beamforming (BF), which is employed at both the access point (AP) and the user equipment (UE) [1]–[6]. However, BF comes with the necessity of accurate beam pointing in order to guarantee perfect transceiver antenna alignment and support UE mobility [7]. As a consequence, several beam-tracking approaches have been presented for directional communication systems operating in lower frequency bands. The problem with adopting the conventional beam-tracking approach is the requirement for an unaffordable pilot overhead [8]. As a result, novel smart beam-tracking schemes are needed to avoid antenna misalignment [9], [10].

Three main beam-tracking approaches for millimeter wave and THz wireless systems have been reported in the open technical literature, namely codebook-based, perturbation and prediction methods (see for example [11]–[15] and references therein). In more detail, in [11], an algorithm that estimates the angle of arrival (AoA) by using variations in the radiation pattern of the beam as a function of the AoA is presented, whereas, in [12], a hierarchical multi-resolution codebook is designed to construct training beamforming vectors with different beamwidths. Likewise, in [13], a Kalman-filter in combination with an abrupt change detection were utilized for pencil-beam tracking, while in [14], an extended Kalman filter was employed that requires only one measurement of the single beam-pair to track the propagation path.

Moreover, in [15], the authors reported a beam-tracking prediction approach, which guarantees high-accuracy with low latency. However, the core assumption of this approach is that the UE follows linear motion. Thus, in a different scenario, this approach fails to provide the required accuracy under a low overhead specification. Finally, in [16], the authors proposed a cooperation-aided prediction-based beam-tracking approach, which relaxes the linearity motion demand of [15].

The disadvantages of the above mentioned approaches are that the codebook-based ones are limited by the resolution of the codebook, whereas the perturbation approaches require lengthy beam training, which incurs large overhead as well as delay. Finally, the prediction approaches suffer from low accuracy and usually support a small set of UE movements. To overcome the aforementioned restrictions, in this paper, a novel hierarchical beam-tracking approach, suitable for THz wireless systems is presented. This approach combines hierarchical codebook search with a location prediction algorithm. Both the hierarchical codebook and the location prediction are used to track the UE with low pilot overhead. The prediction algorithm is based on the observation that all motions can be described as multiple smaller linear motions. Therefore, by increasing the frequency of the direction estimations (estimations/sec), the prediction becomes more accurate. As a result, the tracking algorithm can reduce its pilot overhead significantly. Finally, a hierarchical codebook search is used to improve the efficiency of the algorithm in terms of average number of pilots while also improving the MSE, which are both used to evaluate the performance of the algorithm. The performance of the algorithm is compared with the corresponding performance of the fast channel tracking (FCT) algorithm.

Notations: Unless otherwise stated, lower case and upper case bold letters denote a vector and a matrix, respectively, while \mathbf{A}^H stands for the conjugate transpose, and $\text{tr}(\mathbf{A})$ represents the trace of matrix \mathbf{A} . Finally, \mathbf{I}_K is the $K \times K$ identity matrix.

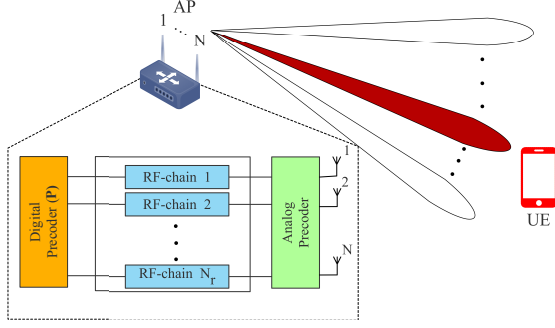


Fig. 1: System model.

II. SYSTEM AND SIGNAL MODEL

As illustrated in Fig. 1, a typical THz massive multiple-input multiple-output (MIMO) system is considered. The AP is equipped with a uniform linear array (ULA) consisting of N elements that are driven by N_r radio frequency (RF) chains, with $N_r \leq N$, in order to serve K single-antenna UEs. In the downlink, the baseband equivalent received signal vector for all the K UEs can be obtained as [15]

$$\mathbf{y} = \mathbf{H}^H \mathbf{W}^H \mathbf{P} \mathbf{s} + \mathbf{z}, \quad (1)$$

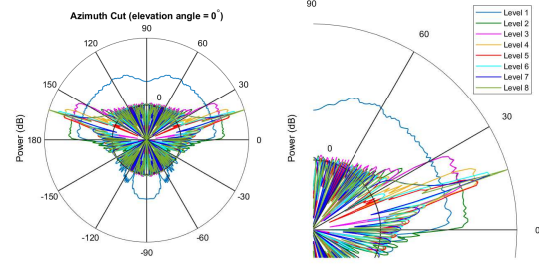
where \mathbf{s} , \mathbf{P} and \mathbf{W} respectively stand for the transmitted signal vector for all the K UEs with normalized power, i.e. $\mathbb{E}[\mathbf{s}\mathbf{s}^H] = \mathbf{I}_K$, the digital precoding matrix and the multi-resolution codebook matrix, while \mathbf{H} and $\mathbf{z} \sim \mathcal{CN}(0, \sigma^2 \mathbf{I}_K)$ denote the MIMO channel matrix and the additive Gaussian noise (AWGN) vector with variance σ^2 , respectively. Of note, the precoding matrix satisfies the total transmit power constraint, i.e. $\text{tr}(\mathbf{P}\mathbf{P}^H) \leq P$, with P being the total transmit power.

Without loss of generality, the multi-resolution codebook designed in [17, Sec.III.C.3] has been considered. Note that this codebook is suitable for an analog beamforming architecture and results in a number of levels equal to $U = \log_2(N)$, with 2^u codewords at each level, where $u = 1, 2, \dots, U$. According to [17, Cor. 1], after the evaluation of the first codeword in each level, the rest of the codewords can be calculated through rotation. An indicative example of the codebook's levels and the corresponding antenna patterns for $N = 256$ and center frequency set to 275 GHz is illustrated in Fig. 2.

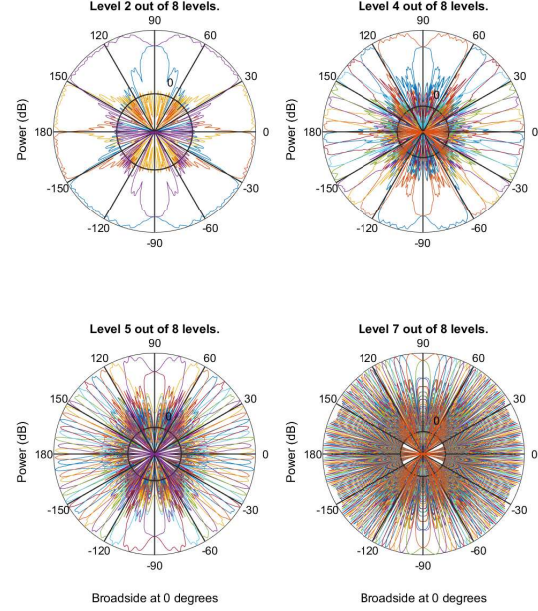
The MIMO channel matrix can be expressed as $\mathbf{H} = [\mathbf{h}_1, \mathbf{h}_2, \dots, \mathbf{h}_K]$, where \mathbf{h}_k is the channel vector corresponding to the k -th UE, with $k = 1, 2, \dots, K$. Adopting the widely-used Saleh-Valenzuela model for the THz channel¹, \mathbf{h}_k can be obtained as

$$\mathbf{h}_k = \beta_k^{(0)} \mathbf{a}(\psi_k^{(0)}) + \sum_{i=1}^L \beta_k^{(i)} \mathbf{a}(\psi_k^{(i)}), \quad (2)$$

¹Notice that the SV model has been extensively used to model indoor environments in wireless THz systems (see e.g. [15], [18] and references therein).



(a) Patterns of matching codewords between the different levels



(b) Patterns of all the codewords within a particular level

Fig. 2: Indicative example of the codebook design.

where $\beta_k^{(0)}$ and $\beta_k^{(i)}$ denote the complex gains of the LoS and non-LoS components, respectively, $\mathbf{a}(\psi)$ stands for the steering vector in the spatial direction ψ , while $\psi_k^{(0)}$ and $\psi_k^{(i)}$ respectively represent the spatial directions of the LoS and non-LoS components. In the THz band, scattering induces more than 20 dB attenuation in the non-LoS components [19]–[24]; hence, only the LoS component can be used reliably. Therefore, (2) can be simplified as $\mathbf{h} \approx \beta \mathbf{a}(\psi)$.

The array steering vector can be expressed as

$$\mathbf{a}(\psi) = \frac{1}{\sqrt{N}} [e^{-j2\pi\psi m}]_{m \in \mathcal{I}(N)}, \quad (3)$$

where $\mathcal{I}(N) = l - (N - 1)/2$, with $l = 0, 1, \dots, N - 1$ stands for a symmetric set of indices centered around zero. Moreover, the spatial direction is connected with the wavelength λ and the inter-element antenna spacing d through $\psi \triangleq \frac{d}{\lambda} \sin(\theta)$, where θ is the actual direction of the UE. Finally, without loss of generality, it is assumed that $d = \lambda/2$.

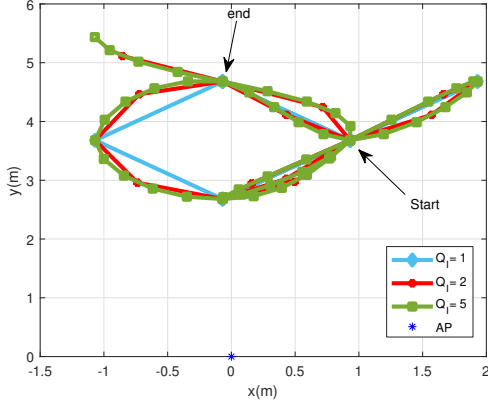


Fig. 3: Random motion with different Q_I .

Note that the UE motions is modeled as a random walk process [25]. The starting locations of the UE are generated uniformly on a disk centered at the room center. The motion of the UE is generated by the random walk process, and is resampled with a factor $Q_I > 1$. The number of timeslots of the resulting motion is Q_I times greater than the original's ($Q_I = 1$). The increase of Q_I is expected to reduce the average number of pilots and MSE. Fig. 3 shows an example of a random motion with different factors Q_I .

III. HIERARCHICAL BEAM-TRACKING APPROACH

For the sake of simplicity, a single UE is considered, i.e. $K=1$. The proposed approach consists of three phases, namely initialization, location prediction, and direction refinement.

A. Phase 1: Initialization

The objective of this phase is to accurately determine three consecutive UE locations, in order for Phase 2 to begin and reduce the pilot overhead to affordable levels. In this sense, during the first three timeslots, a combination of high and low level codewords is used. In each one of these timeslots, the following procedure is employed:

- 1) Level 1 codewords exhaustive search: The AP performs an exhaustive search by switching between the codewords of the first level, which generate the lowest available resolution antenna pattern, in order for the AP to determine the sector in which the UE is located, i.e. the level 1 codeword that should be used to serve the UE.
- 2) Higher level codeword refinement: Afterwards, the AP refines the search by selecting the next higher level of the codebook and switching between those codewords of this level that generate beam patterns within the direction specified in the previous step. Note that these codewords generate narrower beams in comparison with those of the previous level. This step is repeated until the algorithm reaches the highest level of

the codebook. If the algorithm fails to find the direction of the UE for a codebook level, it switches to one level lower and continues the procedure.

- 3) Distance and location estimation: To estimate the transmission distance a two-way time of arrival approach [26] has been employed. The AP-UE distance can be obtained as

$$\tilde{r} = r + e, \quad (4)$$

where r is the actual AP-UE distance and e is a normally distributed random variable with zero mean and standard deviation σ_e [27]. By defining a two-dimensional Cartesian coordinate system, in which the AP is placed at $(0,0)$, as illustrated in Fig. 3, the location of the UE can be estimated as

$$\mathbf{p}(x, y) = (\tilde{r} \cos \tilde{\theta}, \tilde{r} \sin \tilde{\theta}), \quad (5)$$

where $\tilde{\theta}$ is the main lobe direction of the highest level codeword and represents the estimated direction of the UE, while x and y stand for the coordinates.

B. Phase 2: Location prediction

After obtaining the UE's three consecutive locations from Phase 1 and assuming that the UE follows a linear motion, the AP can predict the UE's upcoming location as [16]

$$\mathbf{p}(t+1) = \mathbf{p}(t) + \frac{[\mathbf{p}(t) - \mathbf{p}(t-1)] + [\mathbf{p}(t-1) - \mathbf{p}(t-2)]}{2}, \quad (6)$$

where t refers to the current timeslot. The accuracy of the prediction helps reduce the required pilot overhead as fewer codewords need to be tested by the AP. Therefore, the required pilot overhead can be reduced significantly.

C. Phase 3: Direction refinement

In this Phase, the AP refines the prediction of Phase 2. The AP switches between the codewords of level $U-g$, where $1 \leq g \leq U-3$, that generate beams toward and around the predicted direction, in order to find the UE's direction. Next, it uses the next level to find a more accurate direction, by generating beams towards the direction pointed by the previous level. This is repeated until the last codebook level. The use of multiple codebook levels in this step is expected to increase the robustness of the algorithm, in cases of non-linear motions and non-constant speed, while keeping the pilot overhead low. Finally, the AP repeats step 3 of Phase 1, Phase 2 and Phase 3.

IV. SIMULATION RESULTS & DISCUSSION

In this section, the effectiveness of the proposed approach is evaluated in terms of average number of pilots and $\text{MSE} = \frac{1}{n} \sum_{i=1}^n (\tilde{\theta} - \theta)^2$. The results are derived by means of Monte Carlo simulations in 10,000 different motions generated by the new motion generation. The following insightful scenario is considered. The room dimension is $5 \times 5 \text{ m}^2$, the step of the random motion is 1 m and the number of timeslots is 10 times the value of Q_I . The ULA consists of 256 elements; thus, 8 codebook levels are considered, while the carrier frequency and the signal-to-noise ratio (SNR) are equal to 275 GHz and 10 dB, respectively. The FCT algorithm that was presented in [15], is used as a benchmark. Notice that FCT essentially employs the last codebook level and a prediction based on previous directions. Moreover, it uses 128 pilots in the first 3 timeslots that compose the initialization phase and 16 pilots thereafter. Unless otherwise stated, the number of pilots per codebook level of the proposed approach is 2, in the first 2 levels, and 4 thereafter. Therefore, the total number of pilots in Phase 1 is 28. Phase 3 utilizes the last 4 codebook levels, which result in 16 pilots. Finally, the algorithms restart in the next timeslot if $|\tilde{\theta}(t) - \theta(t)| > \theta_{3dB}$, where θ_{3dB} is the half power beamwidth. Notice that if this condition holds, the communication between the AP and the UE is interrupted.

In Fig. 4, the MSE is illustrated as a function of σ_e , for different number of pilots per codebook level and $Q_I = 10$. The number of pilots per codebook level affects the number of directions searched; hence, the area covered by each level of the codebook during tracking. As a consequence, a low number of pilots covers a small area and limits the effectiveness of tracking in terms of MSE. On the other hand, as the number of pilots increases, the overall tracking overhead also increases. Moreover, from this figure, it is evident that independently of σ_e , approximately the same error performance can be achieved with 4 or 5 pilots per level. Additionally, as the number of pilots per level increases from 3 to 4, MSE decreases for about 0.0133. Finally, the MSE of FCT is 3 times higher than the proposed approach with $\sigma_e = 0 \text{ m}$ and 2.5 times higher with $\sigma_e = 0.5 \text{ m}$.

Fig. 5 depicts the average number of pilots versus Q_I , for different σ_e values. The graph denoted as “Level 8” corresponds to the special case in which only the last codebook level is employed in Phase 3 of the proposed approach with the same total number of pilots. From this figure, we observe that, for a given σ_e , the average number of pilots, when the proposed approach is employed, decreases as Q_I increases. On the other hand, the average number of pilots of the “Level 8” approach and the FCT is almost constant and independent of Q_I . The high average number of pilots of the FCT and “Level 8” approach is related to the estimation error as well as the higher number of pilots that are employed during

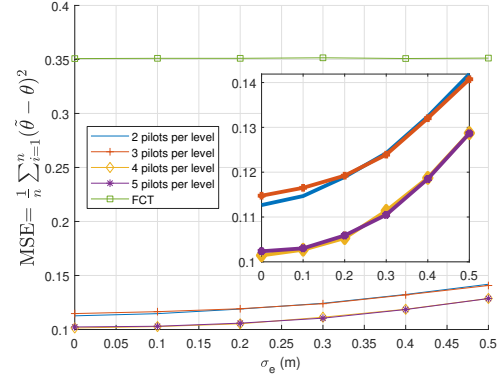


Fig. 4: MSE vs σ_e .

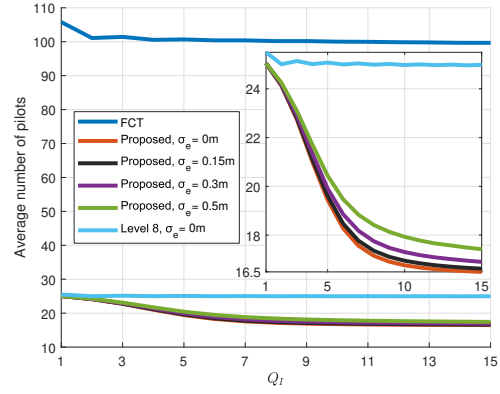


Fig. 5: Average number of pilots vs Q_I .

the initialization phase of FCT. Notice, that according to this result, the average number of pilots for the FCT is between 99.7 and 105.8, while for the “Level 8” approach it is between 25 and 25.5. On the contrary, the average number of pilots for the proposed approach is between 16.5 and 25 with $\sigma_e = 0 \text{ m}$, while it is between 17.4 and 25 with $\sigma_e = 0.5 \text{ m}$. Thus, the use of a hierarchical codebook, makes tracking more robust to direction and speed variations.

V. CONCLUSION

In this paper, a novel hierarchical beam-tracking algorithm for indoor THz communication systems that requires low pilot overhead and provides high tracking efficiency was presented. The proposed approach requires 78.13% less pilot overhead in the initialization phase than the FCT, while the overall overhead reduction that can be achieved by the proposed approach in comparison with the FCT may exceed 76%. Finally, it achieves lower error performance compared to FCT.

ACKNOWLEDGMENT

This work has received funding from the European Commission’s Horizon 2020 research and innovation programme TERRANOVA under grant agreement No. 761794 (TERRANOVA) and No. 871464 (ARIADNE).

REFERENCES

- [1] C. Lin and G. Y. L. Li, "Terahertz communications: An array-of-subarrays solution," *IEEE Commun. Mag.*, vol. 54, no. 12, pp. 124–131, Dec. 2016.
- [2] A.-A. A. Boulgeorgos, A. Alexiou, T. Merkle, C. Schubert, R. Elschner, A. Katsiotis, P. Stavrianos, D. Kritharidis, P.-K. Chartsias, J. Kokkonien, M. Juntti, J. Lehtomaki, A. Teixeira, and F. Rodrigues, "Terahertz technologies to deliver optical network quality of experience in wireless systems beyond 5G," *IEEE Commun. Mag.*, vol. 56, no. 6, pp. 144–151, Jun. 2018.
- [3] E. N. Papatotiriou, A.-A. A. Boulgeorgos, and A. Alexiou, "Performance analysis of THz wireless systems in the presence of antenna misalignment and phase noise," *IEEE Commun. Lett.*, pp. 1–1, 2020.
- [4] A.-A. A. Boulgeorgos and A. Alexiou, "Error analysis of mixed THz-RF wireless systems," *IEEE Commun. Lett.*, vol. 24, no. 2, pp. 277–281, Feb. 2020.
- [5] A.-A. A. Boulgeorgos, S. Goudos, and A. Alexiou, "Users association in ultra dense THz networks," in *IEEE International Workshop on Signal Processing Advances in Wireless Communications (SPAWC)*, Kalamata, Greece, Jun. 2018.
- [6] A.-A. A. Boulgeorgos and A. Alexiou, "Analytical performance evaluation of beamforming under transceivers hardware imperfections," in *IEEE Wireless Communications and Networking Conference (WCNC)*. IEEE, Apr. 2019.
- [7] A.-A. A. Boulgeorgos, A. Alexiou, D. Kritharidis, A. Katsiotis, G. Ntouni, J. Kokkonien, J. Lehtomaki, M. Juntti, D. Yankova, A. Mokhtar, J.-C. Point, J. Machodo, R. Elschner, C. Schubert, T. Merkle, R. Ferreira, F. Rodrigues, and J. Lima, "Wireless terahertz system architectures for networks beyond 5G," *TER-RANOVA CONSORTIUM*, White paper 1.0, Jul. 2018.
- [8] L. Dai, J. Wang, Z. Wang, P. Tsiaflakis, and M. Moonen, "Time domain synchronous OFDM based on simultaneous multi-channel reconstruction," in *IEEE International Conference on Communications (ICC)*, Jun. 2013, pp. 2984–2989.
- [9] A.-A. A. Boulgeorgos and A. Alexiou, *Next Generation Wireless Terahertz Communication Networks*. CRC press, 2020, ch. Antenna misalignment and blockage in THz communications.
- [10] J. Kokkonien, A.-A. A. Boulgeorgos, M. Aminu, J. Lehtomaki, A. Alexiou, and M. Juntti, "Impact of beam misalignment on THz wireless systems," *Nano Commun. Networks*, vol. 24, p. 100302, May 2020.
- [11] K. Gao, M. Cai, D. Nie, B. Hochwald, J. N. Laneman, H. Huang, and K. Liu, "Beampattern-based tracking for millimeter wave communication systems," in *IEEE Global Communications Conference (GLOBECOM)*, Dec 2016, pp. 1–6.
- [12] A. Alkhateeb, O. El Ayach, G. Leus, and R. W. Heath, "Channel estimation and hybrid precoding for millimeter wave cellular systems," *IEEE J. Sel. Topics Signal Process.*, vol. 8, no. 5, pp. 831–846, Oct. 2014.
- [13] C. Zhang, D. Guo, and P. Fan, "Tracking angles of departure and arrival in a mobile millimeter wave channel," in *IEEE International Conference on Communications (ICC)*, May 2016.
- [14] V. Va, H. Vikalo, and R. W. Heath, "Beam tracking for mobile millimeter wave communication systems," in *IEEE Global Conference on Signal and Information Processing (GlobalSIP)*, Dec. 2016.
- [15] X. Gao, L. Dai, Y. Zhang, T. Xie, X. Dai, and Z. Wang, "Fast channel tracking for terahertz beamspace massive MIMO systems," *IEEE Trans. Veh. Technol.*, vol. 66, no. 7, pp. 5689–5696, Jul. 2017.
- [16] G. Stratidakis, A.-A. A. Boulgeorgos, and A. Alexiou, "A co-operative localization-aided tracking algorithm for THz wireless systems," in *IEEE Wireless Communications and Networking Conference (WCNC)*, Marrakech, Morocco, Apr. 2019.
- [17] Z. Xiao, T. He, P. Xia, and X. Xia, "Hierarchical codebook design for beamforming training in millimeter-wave communication," *IEEE Trans. Wireless Commun.*, vol. 15, no. 5, pp. 3380–3392, May 2016.
- [18] A. Sayeed and J. Brady, "Beamspace MIMO for high-dimensional multiuser communication at millimeter-wave frequencies," in *IEEE Global Communications Conference (GLOBECOM)*, Dec. 2013.
- [19] E. N. Papatotiriou, J. Kokkonien, A.-A. A. Boulgeorgos, J. Lehtomaki, A. Alexiou, and M. Juntti, "A new look to 275 to 400 GHz band: Channel model and performance evaluation," in *IEEE 29th Annual International Symposium on Personal, Indoor and Mobile Radio Communications (PIMRC)*. IEEE, Sep. 2018.
- [20] A.-A. A. Boulgeorgos, E. N. Papatotiriou, and A. Alexiou, "Analytical performance assessment of THz wireless systems," *IEEE Access*, vol. 7, no. 1, pp. 1–18, Jan. 2019.
- [21] A.-A. A. Boulgeorgos, E. N. Papatotiriou, and A. Alexiou, "Analytical performance evaluation of thz wireless fiber extenders," in *IEEE 30th Annual International Symposium on Personal, Indoor and Mobile Radio Communications (PIMRC)*, Sep. 2019, pp. 1–6.
- [22] A.-A. A. Boulgeorgos, E. N. Papatotiriou, and A. Alexiou, "A distance and bandwidth dependent adaptive modulation scheme for THz communications," in *19th IEEE International Workshop on Signal Processing Advances in Wireless Communications (SPAWC)*, Kalamata, Greece, Jul. 2018.
- [23] A.-A. A. Boulgeorgos and A. Alexiou, "Performance evaluation of the initial access procedure in wireless THz systems," in *16th International Symposium on Wireless Communication Systems (ISWCS)*, Aug. 2019.
- [24] A.-A. A. Boulgeorgos, E. N. Papatotiriou, J. Kokkonien, J. Lehtomaki, A. Alexiou, and M. Juntti, "Performance evaluation of THz wireless systems operating in 275–400 GHz band," in *IEEE 87th Vehicular Technology Conference (VTC Spring)*. IEEE, Jun. 2018.
- [25] Weisstein, Eric W. "Random Walk–2-Dimensional." From MathWorld–A Wolfram Web Resource. <http://mathworld.wolfram.com/RandomWalk2-Dimensional.html>.
- [26] W. Dargie and C. Poellabauer, *Fundamentals of Wireless Sensor Networks*. John Wiley & Sons, Ltd, Jul. 2010.
- [27] E. Kim and K. Kim, "Distance estimation with weighted least squares for mobile beacon-based localization in wireless sensor networks," *IEEE Signal Processing Letters*, vol. 17, no. 6, pp. 559–562, jun 2010.